HHS Public Access

Author manuscript

Colloids Surf B Biointerfaces. Author manuscript; available in PMC 2018 September 01.

Published in final edited form as:

Colloids Surf B Biointerfaces. 2017 September 01; 157: 490–502. doi:10.1016/j.colsurfb.2017.06.025.

Folic acid conjugated polymeric micelles loaded with a curcumin difluorinated analog for targeting cervical and ovarian cancers

Duy Luong[a,‡], **Prashant Kesharwani**[a,b,‡], **Hashem O. Alsaab**[a,c], **Samaresh Sau**[a], **Subhash Padhye**[d], **Fazlul H. Sarkar**[e], and **Arun K. Iyer**[a,f,*]

[a]Use-inspired Biomaterials & Integrated Nano Delivery (U-BiND) Systems Laboratory Department of Pharmaceutical Sciences, Eugene Applebaum College of Pharmacy and Health Sciences, 259 Mack Ave, Wayne State University, Detroit, MI 48201, USA

[b]Pharmaceutics Division, CSIR-Central Drug Research Institute, Lucknow 226031, India

[c]Department of Pharmaceutics and Pharmaceutical Technology, Taif University, Taif, 26571, Saudi Arabia

[d]Interdisciplinary Science & Technology Research Academy, Department of Chemistry, Abeda Inamdar College, University of Pune, Pune 411001, India

[e]Retired Distinguished Professor, Department of Pathology, Barbara Ann Karmanos Cancer Institute, Wayne State University, School of Medicine, Detroit, Michigan 48201, USA

[f]Molecular Therapeutics Program, Barbara Ann Karmanos Cancer Institute, Wayne State University, School of Medicine, Detroit, Michigan, 48201, USA

Abstract

The current study utilizes folic acid conjugated poly(styrene-co-maleic anhydride) block copolymer (FA-SMA) to enhance the solubility of a hydrophobic but very potent synthetic curcumin-difluorinated (CDF) analog and its targeted delivery to folate receptor-alpha overexpressing cancers. The nanomicelles showed high aqueous solubility. Importantly, the encapsulation of CDF in nanomicelles resulted in high photo-stability of the otherwise photolabile drug. When the nanomicelles were tested in folate-receptor overexpressing ovarian and cervical cancer cells they exhibited high anticancer activity causing significant cell population to undergo apoptosis due to upregulation of tumor suppressor phosphatase and tensin homolog (PTEN) and inhibition of nuclear factor kappa-B (NFκB), which further confirmed the targeting ability and anticancer potentials of folate-targeted formulations.

Graphical Abstract

[*]**Corresponding author:** Arun K. Iyer, Ph.D., Department of Pharmaceutical Sciences, Eugene Applebaum College of Pharmacy and Health Sciences, 259 Mack Ave, Room 3601, Wayne State University, Detroit, MI 48201, Phone: 313-577-5875, Fax: 313-577-2033, arun.iyer@wayne.edu (A.K. Iyer).

[‡]Equally contributing authors

Disclosures: There is no conflict of interest and disclosures associated with the manuscript.

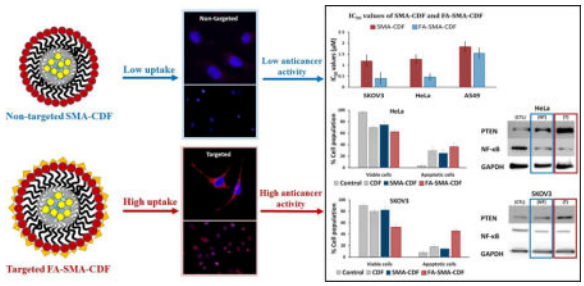

Keywords

Ovarian cancer; cervical cancer; folic acid; folate receptor-alpha targeting; polymeric micelles; curcumin difluorinated (CDF); flavonoid analog; targeted drug delivery

Background

Worldwide, cancer accounts for millions of deaths annually. Chemotherapy, radiotherapy, and photothermal therapy are the most common approaches for cancer treatment. Chemotherapy is a foremost modality for most cancer types because of its high efficacy compared to other treatments [1–3]. Most of the cancer patients are diagnosed at the advanced stage and can only be treated with chemotherapy and radiotherapy. However, development of resistance to conventional chemotherapy is the most common reason for the failure of cancer treatment. In addition, the nonspecific distribution of conventional chemotherapeutic drugs in the body affect both cancerous and normal cells, leading to dose-related adverse effects and insufficient drug concentrations in the cancerous tissues. An ideal delivery carrier for anticancer drugs must be capable of transporting the drug specifically to the cancerous tissues and releasing the drug molecules inside the tumor cells [4–6].

Polymeric nanomicelles have been widely used in medicine as drug delivery carrier by active targeting approach [7–9] They have the ability to improve hydrophobic drug delivery, reducing metabolic drug degradation, specific targeting of cancer cells by surface modification using targeted ligand, and displaying sustained and triggered drug release [10–12]. In addition to the ability to enhance the aqueous solubility of hydrophobic drugs, nanomicelles also have the ability to target cancer cells by two approached: passive and active. The passive targeting ability of nanomicelles takes advantage of the phenomenon called the enhanced permeability and retention (EPR) effect, which was discovered by Matsumura and Maeda. The EPR phenomenon suggested that the proliferation of cancer cells results in the development of the highly disorganized and leaky blood vessels. Thus, the macromolecules including nanomicelles can extravasate and accumulate at the tumor site [12–17]. In the active targeting approach, nanomicelles are typically conjugated/decorated with a targeting moiety, thereby facilitating the preferential accumulation of the drug in selected tissues, individual cancer cells, or intracellular organelles that are associated with specific recognition molecules in cancer cells [14,18–24].

Regarding receptor mediated targeting, folate receptor-alpha targeting by using folic acid seem to be a promising strategy for cancer therapy with numerous of drugs going under

clinical trials at this moment [20]. Folate receptor-alpha, a glycosylphosphatidylinositol anchored cell surface receptor, is overexpressed in the majority of cancer tissues with limited expression in healthy tissues and organs [18]. Folate receptor-alpha is highly expressed in ovarian, cervical, epithelial, brain, breast, kidney, and colorectal tumors [25,26]. Folic acid is small (441 Da), stable over a broad range of temperatures and pH values, inexpensive, and non-immunogenic, and it retains its ability to bind to the folate receptor after conjugation with drugs or diagnostic markers [12]. After folate attaches to the receptors located within clathrin, it is internalized through the endocytotic pathway.

In terms of chemotherapeutic agents, curcumin-difluorinated (CDF), a synthetic flavonoid anticancer compound with 16-fold increased half-life and significantly better anticancer activity as compared to its parent compound curcumin, seems to be a very promising chemotherapeutic agent when tested on pancreatic cancer cells [11,27,28]. Although having such a great potential for anticancer activity, CDF's extremely high hydrophobicity, and water insolubility prevent it from moving further to preclinical and clinical testing. In our previous reports, we successfully overcame CDF's solubility drawback using styrene-maleic acid (SMA) copolymer conjugated with hyaluronic acid (HA) [5,10]. With the presence of both hydrophobic and hydrophilic moieties, SMA could form nano-micelles with peripheral hydrophilic carboxylic groups conjugated with HA to target CD44 receptor overexpressed in pancreatic cancer cells, and hydrophobic styrene moieties facilitated encapsulation of CDF (HA-SMA-CDF). As a result, CDF's solubility was increased dramatically with a significant anticancer activity. HA conjugation gave HA-SMA-CDF the ability to accumulate in MIA PaCa-2 cells resulting in better anticancer activity. With the impressive results of HA-SMA-CDF, the aim of this study was to explore CDF's anticancer activity further using folate-mediated delivery to cervical cancer cells (HeLa) and ovarian cancer cells (SKOV3)(Figure 1) [29–32]. For this purpose, SMA copolymer conjugated with folic acid (FA) as targeting ligand was employed.

Methods

Materials

CDF was synthesized as described earlier [10,11]. Poly(styrene-co-maleic anhydride) (Average MW 1600), N-(3-(dimethylamino) propyl)-N-ethyl carbodiimide hydrochloride (EDC), and 3-[4,5dimethylthiazol-2-yl]-2,5diphenyltetrazolium bromide (MTT) was purchased from Sigma-Aldrich (St. Louis, MO). FA was purchased from Fisher Scientific, Waltham, MA. Guava Nexin Reagent for cell apoptosis kit was purchased from EMD Millipore, Billerica, MA. All other chemicals were of reagent grade and used without any modification.

Preparation of folate-conjugated SMA (FA-SMA) copolymer

FA-SMA copolymer was synthesized using a slightly modified method used earlier [33]. Briefly, FA solution was prepared by dissolving known amounts of FA in $NaHCO_3$ buffer and magnetically stirring for 6 h. In another container, SMA polymer was activated by adding EDC and NHS in of DMSO, and the reaction was allowed to complete for 4 h at room temperature. Then activated SMA solution was added dropwise to the alkaline FA

solution under vigorous stirring and stirred for 24 h at room temperature to synthesize FA-SMA conjugate. Finally, FA-SMA conjugate was purified using Millipore tangential flow filtration (TFF), (Millipore, Milford, MA) by ultrafiltration. Final FA-SMA conjugate was lyophilized, characterized [proton nuclear magnetic resonance spectroscopy (^{1}H NMR) and Fourier transform infrared spectroscopy (FTIR)] after which the products obtained were stored in the freezer until further use.

Fabrication and characterization of FA-SMA-CDF nanomicelles

FA-SMA-CDF nanomicelles were fabricated according to the previously reported method by us with significant modification [10,11]. In short, a known quantity of the freshly synthesized FA-SMA conjugate was dissolved in DI water at RT under magnetic stirring, and the pH was adjusted to 5.0. Dissolved CDF in a minimum quantity of DMSO and added dropwise to the FA-SMA polymer solution. Instantaneous self-assembly of the styrene component of SMA and hydrophobic parts in CDF ensured the formation of nanomicelles. Consequently, EDC was added and stirred in the dark for 30 min to minimize CDF light exposure, and maintained the pH at 5.0. The pH was increased to 10.0 by slow addition of 1 M NaOH till the suspension become clear. Final pH was readjusted to 7.4 using 0.1 M HCl and dialyzed overnight using dialysis membrane (molecular weight cutoff 3.5 kDa, Spectrapor, Spectrum Laboratories, SD) against distilled water to remove free drug (CDF), and lyophilized (Eyela Inc., Tokyo, Japan).

FA-SMA-CDF nanomicelles were characterized for particle size and zeta potential using a Beckman Coulter Delsa Nano-C DLS Particle analyzer (Beckman Coulter, Inc., Fullerton, CA) equipped with a 658 nm He–Ne laser as reported earlier by us [5,10,11]. Subsequently, nanomicelles were further characterized for surface morphology by transmission electron microscopy (TEM) and atomic force microscopy (AFM) as reported earlier [11].

Drug loading study

The amount of drug present in the nanomicelles was determined by High-performance liquid chromatography (HPLC) method using a C18 column with Photodiode Array detector (PDA) at 447 nm. For this purpose, initially, the standard curve of CDF was first performed by dissolving the known amount of CDF in DMSO and its successive dilutions (in mobile phase), followed by HPLC analysis with the absorbance at 447 nm. Further, the amount of CDF loading in micelles was calculated by dissolving the known amount of micelles in PBS buffer (pH 7.4) followed by further dilution in the mobile phase and determination of CDF loading by HPLC at the absorbance at 447 nm against the standard curve.

Stress stability indication assay

Free CDF, SMA-CDF, and FA-SMA-CDF nanomicelles were exposed to different stress conditions such as thermal, acid, alkaline, oxidation, and photolytic in order to generate degradation byproducts of the drug. These conditions included heat (95°C), acid hydrolysis (1N hydrochloric acid), base hydrolysis (1N sodium hydroxide solution), oxidation (3% hydrogen peroxide solution), and photolysis with UV light. Samples were later analyzed by HPLC to ensure that there was no interference between the degradation products and pure drug peak.

Cell culture

Human cervical cancer cells (HeLa cells), human ovarian carcinoma cells (SKOV3 cells) (folate receptor overexpressing cell lines) [29–31,34], and human lung cancer cells (A549 cells) (folate receptor negative cell line) [35,36] were used in this study. HeLa cells were cultured in Dulbecco's Modified Eagle's Medium (DMEM; Fisher Scientific, Waltham MA). SKOV3 cells were cultured in Roswell Park Memorial Institute (RPMI) 1640 Medium (Thermo Fisher Scientific, USA). A549 cells were cultured in Kaighn's Modification of Ham's F-12 Medium (F-12K; Thermo Fisher Scientific, USA). All media contained 10% fetal bovine serum (FBS) and streptomycin sulfate (10mg/L). All cell lines were incubated at 37°C in a 5% CO_2 air humidified atmosphere.

In vitro cytotoxicity assay

The *in vitro* cytotoxicity of free CDF, SMA-CDF and FA-SMA-CDF nanomicelles was evaluated by MTT assay on HeLa, SKOV3, and A549 (negative control) cell lines. In short, cells were seeded in 96-well plates with an average of 2000 cells in each well. After 24 h incubation, cells were treated with various formulations with a concentration range from 0.5 μM – 2 μM. Treated cells were incubated for 72 h at 37°C, followed by addition of MTT solution (1 mg/ml) and further incubation at 37°C for 2 h. Following this, media was replaced by DMSO and the plates were placed on a shaker for 10 mins. The absorbance was measured at 590 nm using a high-performance multi-mode plate reader (Synergy 2, BioTek). Percentage of survival cells was determined by comparing the absorbance with appropriate controls [10,11].

Fluorescence microscopic studies

Fluorescence microscopic study was performed in SKOV3 cell line (folate receptor overexpressing cell line) to examine the effect of folate receptor targeting ability of the targeted formulation on cellular internalization as compared to the non-targeted formulation. In brief, SKOV3 cells (5×10^4) were seeded in four-well chamber slide and incubated at 37°C under 5% CO_2 for 24 h. The medium was removed, and Rhodamine B loaded formulations (non-targeted and targeted) were added and incubated for 6 h. The formulation containing medium was removed, and resulting cells were washed with PBS three times and fixed with 3% formaldehyde in the PBS at RT for 10 min, and the samples were analyzed qualitatively using a fluorescent microscope (Leica, Germany) [37].

Confocal microscopic study

SKOV3 cells were seeded in a four-well chamber slide at a density of 1×10^4 cells in a total volume of 400 μl for each well and allowed to incubate overnight. Media was replaced with formulations loaded with Rhodamine B and incubate for 6 h. Following, the supernatant was, and cells were washed thrice with 400 μl of PBS. Then, cells were fixed with 3% paraformaldehyde solution in PBS for 10 min at room temperature. This solution was then discarded, and cells were washed thrice with 400 μl of PBS. The nucleus was stained with a cell permeable far-red fluorescent DNA dye DRAQ5® (Cell Signaling Technology, USA) at a concentration of 5 μM for 10 min at room temperature. Cells were then washed thrice with 400 μl of PBS. The chambers were then removed, and 1 drop of mounting media (Thermo

Fisher Scientific) was added per coverslip. The coverslips were mounted on the slide and let sit for 1 h in the dark. Images were recorded using Leica TCS SP5 confocal microscope.

Western blot

Western blot analysis was performed to determine the level expression of Phosphatase and tensin homolog PTEN and Nuclear factor kappa B (NF-κB) in HeLa and SKOV3 cell line using reported method [38]. Briefly, HeLa and SKOV3 cells were treated with different nanoformulations and lysed. The protein concentration was determined by the Bio-Rad Protein Assay (Bio-Rad kit). Lysates were electrophoresed by SDS-PAGE and the proteins were transferred onto the nitrocellulose blotting membrane, followed by blocking with 5% BSA in TBST buffer at room temperature for 1h. Primary antibodies (PTEN or NF-κB) were added and incubated overnight at 4°C, subsequently washed and incubated with compatible secondary antibodies. The protein bands were visualized by incubation with chemiluminescent substrate (Thermos Scientific) at room temperature for 2 min, followed by chemiluminescent detection using a digital imaging system (ImageQuant LAS 4000, GE Healthcare Bio-Sciences AB, Sweden).

Flow cytometry

HeLa cells and SKOV3 cells were cultured in 6-well plates at 50000 cells/well and incubated for 24 h at 37°C under 5% CO_2, followed the treatment of plain CDF, SMA-CDF, and FA-SMA-CDF to induce apoptosis. The concentrations of CDF, SMA-CDF, and FA-SMA-CDF were chosen based on the value of IC_{50} on HeLa cells and SKOV3 cells from *in vitro* cytotoxicity assay. After 72h incubation, cells were collected, and samples were prepared according to the protocol for Guava Nexin Annexin V assay (EMD Millipore, USA). The samples were analyzed by Guava Easycyte flow cytometer (EMD Millipore, USA).

Results

Folate receptor is overexpressed in the vast majority of cancer cells, while its expression is limited in healthy non-target tissues and organs [18]. Also, our earlier studies showed that folate engineered nanocarrier showed promising activity against various cancers. CDF has been shown to be a very promising anticancer agent with the potential to treat several cancer cells as well as overcome drug resistance. However, photolytic decomposition and low solubility profile of CDF has caused difficulties in sample preparation and made its systemic administration problematic. Our earlier reports suggested that SMA based micelles could enhance the solubility of various compounds and satisfy the need to achieve anticancer drug accumulation at the tumor site and minimize adverse side effects [5]. Based on this information, the goal of this work was to design an efficient folate-based targeted nanomicelles system loaded with CDF which could be useful for targeted anticancer therapy for multiple cancers.

Synthesis and characterization of FA-SMA conjugate

FA engineered styrene maleic acid polymer (FA-SMA) was synthesized, purified, and structurally characterized by ^{1}H NMR and FTIR spectroscopy. The ^{1}H NMR spectrum

showed characteristic peaks between 6.85 – 7.60 ppm are ascribed to the benzene unit of folate, and the signal at 8.63 ppm corresponds to the C–H group of the folate nitrogen ring. The characteristic aromatic peaks of the styrene subunits (of SMA) at about 6.2–7.2 ppm further confirmed the presence of SMA components in HA-SMA conjugates. Additionally, the FTIR spectrum of FA-SMA revealed a unique characteristic peak at 1630.71 cm^{-1} was confirmed the formation of an amide bond (Figure 2a).

Fabrication and characterization of drug loaded non-targeted (SMA-CDF) and targeted (FA-SMA-CDF) nanomicelles

DLS was employed for the measurement of the particle size and size distribution of nanomicelles. The obtained particle size and the size distribution of the SMA-CDF nanomicelles were 183.4 ± 3.28 nm and 0.191 ± 0.028, respectively. However, the particle size and the size distribution of the FA-SMA-CDF nanomicelles were 191.3 ± 2.92 nm and 0.176 ± 0.069, respectively (Figure 2b). Both, non-targeted and targeted nanoformulations had a negative zeta potential values of −50.79 ± 1.06 mV and −7.86 ± 1.67 mV, respectively, as measured after dilution with 1 mM NaCl at 25 °C (Figure 2c).

The surface morphology of SMA-CDF and FA-SMA-CDF was investigated by AFM (Figure 3). To investigate the surface morphology of developed nanomicelles, we also performed AFM measurements by immobilizing them on freshly cleaved mica. The spherical shaped nanoparticles were observed using AFM, and FA-SMA-CDF showed comparatively, higher particle size and results have corroborated the results obtained by DLS.

Drug loading in nanomicelles

The loading of the drug in the nanomicelles was estimated by HPLC method. A calibration curve was developed in a range of 10–250 μg/ml (R2 = 0.99) and accuracy and precision data were determined, and the validated HPLC method was employed for determining the CDF concentration and to evaluate drug release from the developed nanomicelles. The loading of CDF in SMA-CDF and FA-SMA-CDF was 18.48 ± 2.79 and 10.44 ± 3.16 % w/w, respectively. The lesser loading of the drug in FA-SMA-CDF may be attributed to the physical interaction between SMA and 1,3 diketonic compounds such as CDF.

Stress stability indication assay

It is illustrated in (Figure 4a) that there is no interference between drug peak and the degradation peaks. Also, by making a nano-micellar formulation for CDF using FA-SMA, the photolysis stability of CDF was increased to a large extent (Figure 4b).

In vitro cancer cell viability assay

CDF loaded nanoformulation cytotoxicity assay was performed against three different types of cell lines [SKOV3 (human ovarian carcinoma cell line), HeLa cells (human cervical cancer cells), and A549 (human lung cancer cells)] in order to determine the efficacy of developed formulations against different types of cancers. Plain polymer (FA-SMA) showed very little toxicity to all the experimental cell lines with the cell viability more than 90%, confirmed the safety of the carriers. The anticancer activity of FA-SMA-CDF nanomicelles

was compared with SMA-CDF and the free drug. Targeted nanomicelles exhibited an improvement in anticancer activity in all three experimental cells after incubation for 72 h with respect to the free drug and non-targeted nanomicelles.

For cytotoxicity assay, different cells were treated with four equivalent doses of CDF; 0.5, 1, 1.5, and 2 μM of the formulations. The result of the MTT cell viability assay exhibited a significant difference in the toxicity of folate-based nanomicelles in comparison to plain drug and the non-targeted formulation. FA decorated micelles resulted in a statistically significant enhancement ($P < 0.01$) in the anticancer activity (Figure 5). In SKOV 3 cells, after 72h, half minimal (50%) inhibitory concentration (IC_{50}) values of CDF, SMA-CDF and FA-SMA-CDF were found to be 0.65 ± 0.18, 1.20 ± 0.25, and 0.40 ± 0.26 μM, respectively. FA-SMA-CDF micelles reduced the IC_{50} value of SMA-CDF by approximately 3 folds. A similar pattern of cell viability was observed in the case of HeLa cells, where the IC_{50} values of CDF, SMA-CDF, and FA-SMA-CDF were found to be 0.70 ± 0.26, 1.28 ± 0.19, and 0.47 ± 0.14 μM, respectively after 72h. FA-SMA-CDF micelles reduced the IC_{50} value of SMA-CDF by approximately 2.72 folds.

In the case of A549 cells after 72h, the IC_{50} values of CDF, SMA-CDF, and FA-SMA-CDF were found to be 1.65 ± 0.16, 1.85 ± 0.22, and 1.55 ± 0.23 μM, respectively. FA-SMA-CDF micelles reduced the IC_{50} value of SMA-CDF by approximately 1.19 folds. In this case (A549 cells) the IC_{50} values were comparatively higher than other two experimental cell lines (SKOV3 and HeLa cells).

Fluorescence microscopic study

SKOV3 cells were selected for in vitro fluorescence microscopic study based on the results of MTT and receptor blockade assay. In cell uptake studies, SKOV3 cells were incubated with Rhodamine B labeled formulations and analyzed after 6 h. As shown in Figure 6a, free Rhodamine B treated cells did not show any apparent fluorescence. However, the cells treated with Rhodamine B based nanomicelles were found to be more fluorescent. As compare to non-targeted micelles, comparatively, higher uptake was observed in cells treated with targeted micelles.

Confocal microscopic study

The uptake of the formulation was further confirmed by using confocal microscopic assay using SKOV3 cell lines. After incubating the cells with the formulation for 6 h, they were analyzed under a confocal microscope. As shown in Figure 6b, targeted formulation showed comparatively higher uptake than the non-targeted formulation in both the cell lines. The results are well in accordance with the fluorescence microscopic study indicating the higher cellular uptake of the targeted formulation.

Flow cytometry

Apoptosis induction in HeLa and SKOV3 cells of the drug-loaded formulations was determined by flow cytometry with Annexin V/7-AAD dual staining. The percentage of Annexin V^{-}/7-AAD $^{-}$ (R5), Annexin V^{+}/7-AAD $^{-}$ (R6) and Annexin V^{-}/7-AAD $^{+}$ (R4) and Annexin V^{-}/7-AAD $^{+}$ (R3) were used to determine the number of live cells, early apoptotic,

late apoptotic and necrotic cells. In both HeLa and SKOV3 cell lines, the number of apoptotic cells was found to be significantly higher with targeted formulation FA-SMA-CDF as compared to plain CDF or non-targeted formulation SMA-CDF. The percentage of apoptotic cells were found to be approximately 36.6 ± 6.8 and 45.9 ± 5.4 in targeted formulation FA-SMA-CDF as compared to non-targeted formulation SMA-CDF 25.1 ± 7.5 and 14.5 ± 6.2 in HeLa and SKOV3, respectively. The results suggested a better apoptosis induction ability of targeted formulation FA-SMA-CDF and were consistent with higher anticancer activity in *vitro* cytotoxicity assay using MTT and better cellular uptake in fluorescence and confocal microscopy studies. Besides, plain carrier FA-SMA conjugate exhibited relatively low apoptosis in both HeLa and SKOV3 cell lines, showing its safety when using for drug delivery (Figure 7).

Western blot

Western blot was performed to identify the level of PTEN and NF-κB expression in HeLa and SKOV3 cells after treatment with the nanomicelles. In control cells, PTEN expression was found to be relatively low. However, a significant increase in PTEN level was observed after treatment with nanomicelles. FA-SMA-CDF formulation shown significantly higher increment in PTEN level than SMA-CDF nanomicelles. When it comes to NF-κB expression, in control cells without treatment, NF-κB level was found to be higher than in cells treated with nanomicelles. Noticeably in HeLa cells, the ability to upregulate PTEN and downregulate NF-κB of the formulations is significant (Figure 8).

Discussion

Our newly developed CDF, have shown enhanced stability, higher therapeutic potential, and 16-fold increased half-life compared to conventional curcumin. CDF also displayed extremely enhanced pancreas selective accumulation [28,39]. More importantly, we found that CDF could inhibit the growth of CSCs and induce disintegration of colonospheres that are highly enriched in CSCs [40]. Very recently, our CDF nanoformulations [SMA-CDF, HA-SMA-CDF (hyaluronic acid conjugated SMA-CDF), PAMAM-CDF and HA-PAMAM-CDF] have shown significant activity for the treatment of pancreatic cancers [5,10,11]. Hence we assume that our CDF nanoformulations can be a promising platform for treating CD44 expressing pancreatic cancer stem-like cells (CSLCs).

Based on these promising results of CDF and its nanoformulations, our next challenge was to develop a new CDF based nanoformulation which can be utilized for the treatment of multiple cancers. Because folate receptor-alpha is overexpressed in various cancers such as ovarian, cervical, epithelial, brain, breast, kidney, and colorectal tumors [25,26], we utilized FA as targeting ligand.

Initially, FA-SMA conjugates were synthesized and characterized by ^{1}H NMR and FTIR spectroscopy (Figure 2a). Next, we successfully formulated non-targeted (SMA-CDF) and targeted (FA-SMA-CDF) nanomicelles. The FA present on FA-SMA is hypothesized to form the corona of the nanomicelles, with the ability to bind effectively to various receptors overexpressed on different cancer cells.

We have analyzed our nanomicelles for size, size distribution, charge, and morphology by DLS, and AFM techniques. Our results revealed that formulated nanomicelles were in the ideal size range with narrow size distribution profiles (PDI) for tumor targeting. DLS data suggested that there was a slight increase in particle size following conjugation with folate (FA-SMA-CDF). The increase in particle size was attributed to the bulkiness provided by folate moiety to the nanomicelles. Also, it should be noted that our nanomicelles displayed unimodal size distribution as shown in Figure 2b. Further, AFM images proved them to be in spherical shape and higher particle size for FA-SMA-CDF than SMA-CDF which are well in agreement with results obtained by DLS. Zeta potential data showed negative value and indicating them to be safe carriers for systematic drug delivery (Figure 2c) [41]. Noticeably, the high negative charge of SMA-CDF was neutralized by FA conjugation, resulting in a relatively low negative charge of FA-SMA-CDF nanomicelles. The low negative charge is believed to help the targeted nanomicelles FA-SMA-CDF have lower uptake and less cytotoxicity in phagocytic cells [42].

In regard to the loading of CDF into the micelles, FA-SMA-CDF showed less CDF loading than SMA-CDF formulation. The possible reason was due to the steric hindrance caused by the additional crowding of the ligand on the periphery of the folate-based micelles which prevented CDF from reaching into the micelles core. Another reason was due to the comparatively greater sealing of micelles structure by FA-SMA-CDF at the peripheral portions of micelles as a coating, which prevented CDF loading.

Besides the aqueous solubility issue, CDF is highly prone to photolysis. Because of this susceptibility to photolysis, CDF can lose its anticancer activity dramatically when exposed to light resulting in low cancer treatment efficacy. Fortunately, nanomicelle formation with FA-conjugated SMA does not only enhance CDF's aqueous solubility, deliver CDF specifically to cancer cells but also protect CDF from photolysis. Therefore, the activity of CDF will be retained during the preparation of FA-SMA-CDF formulation prior to intravenous injection. Stability assay showed an approximately 80% of therapeutically active CDF remained in the nanomicelle formulations when exposed to UV stress condition continuously for 2 h. It has been reported that curcumin derivative (CDF) is photolytic unstable and expose of UV light destabilizes the CDF[43]. Noticeably, approximately 90% of plain CDF was decomposed under the same UV stress condition (Figure 4a and b). The results suggested the ability of nanomicelle formulation to enhance the stability of CDF against photolysis.

Human ovarian carcinoma cell line SKOV3, cervical cancer cell line HeLa (folate receptor-alpha-positive control) and human lung cancer cell line A549 (folate receptor deficiency control) were chosen for the *in vitro* cytotoxicity assay. From the *in vitro* cell viability assay (Figure 5), the targeted formulation FA-SMA-CDF showed a significant increase in anticancer activity with a decrease in IC_{50} when tested on SKOV3 and HeLa as compared to non-targeted formulation SMA-CDF. In SKOV3, IC_{50} values after 72h incubation were found to be 1.20 ± 0.25 and 0.40 ± 0.26 μM for non-targeted formulation SMA-CDF and targeted formulation FA- SMA-CDF, respectively. The results observed in HeLa also showed a better anticancer activity of targeted formulation FA-SMA-CDF with IC_{50} of 0.47 ± 0.14 μM as compared to non-targeted formulation SMA-CDF with IC_{50} of 1.28 ± 0.19

μM. On the other hand, in A549 cell line with low expression of folate receptor-alpha, there was a small increase in anticancer activity of targeted formulation FA-SMA-CDF with IC_{50} of 1.55 ± 0.23 μM as compared to the non-targeted formulation SMA-CDF with the IC_{50} value of 1.85 ± 0.22 μM. The higher anticancer activity of FA decorated nanomicelles FA-SMA-CDF found in SKOV3 and HeLa with overexpression of folate receptors as compared to non-targeted formulation SMA-CDF suggested a higher cellular uptake of targeted formulation FA-SMA-CDF in those cell lines. Folate receptor mediated endocytosis helped FA-SMA-CDF internalize faster in SKOV3 and HeLa following by CDF release. Meanwhile, in A549 with low expression of folate receptors, targeted formulation FA-SMA-CDF has a slight increase in activity. This could be explained by the low number of folate receptors on the membrane of A549 cells; therefore, targeted formulation FA-SMA-CDF could not take advantage of folate receptor mediated endocytosis. Interestingly, in all three cell lines, the targeted formulation FA-SMA-CDF showed higher activity than plain CDF. The results suggested the potential of targeted nanomicelles (FA-SMA-CDF) in not only enhancing CDF's poorly aqueous solubility but also improving cellular uptake with better activity. The results also suggested the safety profile of FA-SMA for drug delivery with almost close to 100% cell viability in all three cell lines after 72h incubation. In figure 6a & b, we observed that FA-targeted micelle has higher cell uptake than the non-targeted formulation, which indirectly proves FR-mediated cell uptake. Previously, our lab has shown FR-competition experiment with various types of nanoparticles to prove the receptor mediated uptake [44–46]. Herein, we used folic acid conjugated polymeric micelles, thus one can expect FA-SMA micelle will follow FR-mediated endocytosis and there will be FR-competition.

In fluorescence and confocal microscopic studies, SKOV3 cells were chosen to represent the folate receptor overexpressing cell lines to examine the ability of the targeted formulation FA-SMA-CDF in increasing cellular uptake utilizing folate receptor mediated endocytosis. The majority of receptor mediated uptake is clathrin mediated endocytosis. Due to this, clathrin-mediated endocytosis is historically referred to as "receptor-mediated endocytosis [47]. This is also applicable to folic acid decorated polymer nanoparticles that are first up taken by FR and form "clathrin pit", then they internalize to the cytoplasm and release cargo, and finally FR again recycles back to the cell membrane [15].

It is has been reported that tumor cells over-expressed FR, whereas healthy cells expressed reduced folate carrier (RFC) and the binding affinity of folic acid (FA) to RFC is much weaker than binding affinity between FA and FR [48]. Therefore, FA-conjugated polymer nanoparticles showed high affinity to cancer cells than the normal cells and this is reason FR is a successful biomarker for selective cancer therapy. The formulations were labeled with Rhodamine B, followed by incubation with SKOV3 cells for 6h. The results showed a significantly higher Rhodamine B fluorescence signal in SKOV3 with targeted-formulation FA-SMA-CDF labeled Rhodamine B as compared to non-targeted formulation SMA-CDF labeled Rhodamine B (Figure 6). In combination with the *in vitro* cell viability assay results, the fluorescence, and confocal microscopic studies suggested that the significantly higher anticancer activity of targeted formulation FA-SMA-CDF found in SKOV3 and HeLa were due to the higher cellular uptake facilitated by folate receptor mediated endocytosis.

With results from *in vitro* cell viability assay, fluorescence and confocal microscopic studies, apoptosis assay and western blot studies were performed to further investigate the anticancer potential of CDF in the targeted formulation FA-SMA-CDF against SKOV3 and HeLa cells. Apoptosis assay revealed a higher percentage of apoptotic and necrotic cells in both HeLa and SKOV3 after treatment with targeted formulation FA-SMA-CDF as compared to non-targeted formulation SMA-CDF and plain CDF. The results were in accordance with *in vitro* cell viability assay with a lower percentage of viable cells observed in SKOV3 and HeLa after treatment with FA-SMA-CDF. The higher number of apoptotic and necrotic cells in SKOV3 and HeLa treated with FA-SMA-CDF could be explained by higher uptake of the targeted formulation due to the folate receptor mediated endocytosis. Noticeably, the plain targeted carrier FA-SMA showed a negligible percentage of apoptotic and necrotic cells in both SKOV3 and HeLa cells which indicated that plain FA-SMA is biologically safe and biocompatible at tested concentrations (Figure 7).

Western blot analysis was performed to evaluate the expression levels of tumor suppressor Phosphatase and Tensin homolog PTEN and Nuclear factor – κB (NF-κB) in control and treated SKOV3 and HeLa cells. CDF is known to upregulate PTEN which has been shown to be an important factor in stem cell self-renewal [49–51]. In various human tumors, PTEN downregulation is believed to be the leading factor to the development of chemotherapy resistance and recurrence of cancer by dephosphorylating phosphatidylinositol 3,4,5-trisphosphate (PIP3) and antagonizing the PI3-K/Akt pathway [52]. PTEN also regulates many important processes in cancer cells such as cell proliferation, adhesion, migration, invasion, and apoptosis [38]. From western blot studies, all of the formulations showed an elevated level of PTEN in both SKOV3 and HeLa cells. More importantly, the targeted formulation FA-SMA-CDF showed a higher level of PTEN expression in both SKOV3 and HeLa as compared to non-targeted formulation SMA-CDF and plain CDF. PTEN levels in cells treated with the targeted formulation were found to be higher approximately 1.8 and 2 folds than cells treated with the non-targeted formulation in SKOV3 and HeLa, respectively. Noticeably, as compared to the control without treatment, PTEN expression was elevated by approximately 3 or 6 times after treatment with the targeted formulation in SKOV3 and HeLa, respectively. The same pattern was also observed with NFκB when tested on both SKOV3 and HeLa cells. CDF is a flavonoid analog of curcumin which is known to have the pro-apoptotic properties mediated by downregulation of NFκB in many types of cancer [53,54]. NFκB has been known to induce cell survival through promoting expression of anti-apoptotic genes such as *bcl-x*L [55] and X-linked inhibitor of apoptosis (*XIAP*) [56]. Activation of NFκB has been observed in several types of cancer and is believed to contribute to apoptosis resistance of those cancer cells [57,58]. From western blot results, our formulation showed the ability to downregulate NFκB in both SKOV3 and HeLa cells. FA-SMA-CDF showed a stronger downregulation of NFκB in SKOV3 and HeLa as compared to SMA-CDF. Noticeably in HeLa, the downregulation of NFκB when cells were treated with FA-SMA-CDF is approximately 2 times stronger as compared to SMA-CDF. This results can be attributed to a higher cellular internalization of the targeted formulation FA-SMA-CDF in SKOV3 and HeLa due to the targeting ability of folic acid and followed by sustained release of CDF into the cells (Figure 8). The results suggested the potential of targeted nanomicelles (FA-SMA-CDF) to upregulate the expression of PTEN and

downregulate NFκB which plays an important role in tumor suppressor activity and lead to cancer cell death. In conclusion, FA-conjugated copolymer SMA showed great potential for targeting delivery of CDF, a potent anticancer compound. The FA engineered nanomicelles possess numerous of excellent characteristics such as high CDF loading with the ability to deliver a high dose of CDF to cancer cells utilizing folate receptor mediated endocytosis, enhance CDF's stability against photolysis and biologically safe and biocompatible. Moreover, the targeted formulation FA-SMA-CDF showed the ability to increase the number of apoptotic and necrotic cells, and upregulate level of PTEN expression which is believed to help avoid drug resistance and cancer recurrence after initial treatment. The results suggested the promising potential of FA-SMA-CDF for targeted anticancer therapy, warranting further in vivo investigations underway in our laboratory.

Acknowledgments

The authors wish to acknowledge the funding support from National Cancer Institute's (NCI's) grant 1R21CA179652-01A1. We acknowledge partial support for this work by Wayne State University Start-up funding to A.K.I. We also acknowledge Dr. Guangzhao Mao's group at College of Engineering, Wayne State University, for assistance with AFM analysis.

References

1. Mura S, Nicolas J, Couvreur P. Stimuli-responsive nanocarriers for drug delivery. Nat Mater. 2013; 12:991–1003. DOI: 10.1038/nmat3776 [PubMed: 24150417]
2. Peer D, Karp JM, Hong S, Farokhzad OC, Margalit R, Langer R. Nanocarriers as an emerging platform for cancer therapy. Nat Nanotechnol. 2007; 2:751–760. DOI: 10.1038/nnano.2007.387 [PubMed: 18654426]
3. Mahor A, Prajapati SK, Verma A, Gupta R, Iyer AK, Kesharwani P. Moxifloxacin loaded gelatin nanoparticles for ocular delivery: Formulation and in-vitro, in-vivo evaluation. J Colloid Interface Sci. 2016; 483:132–138. DOI: 10.1016/j.jcis.2016.08.018 [PubMed: 27552421]
4. Maeda H, Wu J, Sawa T, Matsumura Y, Hori K. Tumor vascular permeability and the EPR effect in macromolecular therapeutics: A review. J Control Release. 2000; 65:271–284. DOI: 10.1016/S0168-3659(99)00248-5 [PubMed: 10699287]
5. Kesharwani P, Xie L, Banerjee S, Mao G, Padhye S, Sarkar FH, Iyer AK. Hyaluronic acid-conjugated polyamidoamine dendrimers for targeted delivery of 3,4-difluorobenzylidene curcumin to CD44 overexpressing pancreatic cancer cells. Colloids Surfaces B Biointerfaces. 2015; 136:413–423. DOI: 10.1016/j.colsurfb.2015.09.043 [PubMed: 26440757]
6. Kesharwani P, Iyer AK. Recent advances in dendrimer-based nanovectors for tumor-targeted drug and gene delivery. Drug Discov Today. 2015; 20:536–547. DOI: 10.1016/j.drudis.2014.12.012 [PubMed: 25555748]
7. Wickens JM, Alsaab HO, Kesharwani P, Bhise K, Amin MCIM, Tekade RK, Gupta U, Iyer AK. Recent advances in hyaluronic acid-decorated nanocarriers for targeted cancer therapy. Drug Discov Today. 2016
8. Sahu P, Kashaw SK, Jain S, Sau S, Iyer AK. Assessment of penetration potential of pH responsive double walled biodegradable nanogels coated with eucalyptus oil for the controlled delivery of 5-fluorouracil: In vitro and ex vivo studies. J Control Release. 2017; 253:122–136. [PubMed: 28322977]
9. Bhise K, Kashaw SK, Sau S, Iyer AK. Nanostructured Lipid Carriers Employing Polyphenols as Promising Anticancer Agents: Quality by Design (QbD) approach. Int J Pharm. 2017
10. Kesharwani P, Banerjee S, Padhye S, Sarkar FH, Iyer AK. Hyaluronic Acid Engineered Nanomicelles Loaded with 3,4-Difluorobenzylidene Curcumin for Targeted Killing of CD44+ Stem-Like Pancreatic Cancer Cells. Biomacromolecules. 2015; 16:3042–3053. DOI: 10.1021/acs.biomac.5b00941 [PubMed: 26302089]

11. Kesharwani P, Banerjee S, Padhye S, Sarkar FH, Iyer AK. Parenterally administrable nano-micelles of 3,4-difluorobenzylidene curcumin for treating pancreatic cancer. Colloids Surfaces B Biointerfaces. 2015; 132:138–145. DOI: 10.1016/j.colsurfb.2015.05.007 [PubMed: 26037703]
12. Amjad MW, Amin MCIM, Katas H, Butt AM, Kesharwani P, Iyer AK. *In Vivo* Antitumor Activity of Folate-Conjugated Cholic Acid-Polyethylenimine Micelles for the Codelivery of Doxorubicin and siRNA to Colorectal Adenocarcinomas. Mol Pharm. 2015; 12:4247–4258. DOI: 10.1021/acs.molpharmaceut.5b00827 [PubMed: 26567518]
13. Torchilin VP. Delivery of protein and peptide drugs in cancer. World Scientific. 2006
14. Iyer AK, Singh A, Ganta S, Amiji MM. Role of integrated cancer nanomedicine in overcoming drug resistance. Adv Drug Deliv Rev. 2013; 65:1784–1802. [PubMed: 23880506]
15. Iyer AK, Greish K, Seki T, Okazaki S, Fang J, Takeshita K, Maeda H. Polymeric micelles of zinc protoporphyrin for tumor targeted delivery based on EPR effect and singlet oxygen generation. J Drug Target. 2007; 15:496–506. DOI: 10.1080/10611860701498252 [PubMed: 17671896]
16. Iyer AK, Khaled G, Fang J, Maeda H. Exploiting the enhanced permeability and retention effect for tumor targeting. Drug Discov Today. 2006; 11:812–818. DOI: 10.1016/j.drudis.2006.07.005 [PubMed: 16935749]
17. Amjad MW, Kesharwani P, Amin MCIM, Iyer AK. Recent advances in the design, development, and targeting mechanisms of polymeric micelles for delivery of siRNA in cancer therapy. Prog Polym Sci. 2017; 64:154–181.
18. Yoo HS, Park TG. Folate-receptor-targeted delivery of doxorubicin nano-aggregates stabilized by doxorubicin-PEG-folate conjugate. J Control Release. 2004; 100:247–56. DOI: 10.1016/j.jconrel.2004.08.017 [PubMed: 15544872]
19. Yang X, Singh A, Choy E, Hornicek FJ, Amiji MM, Duan Z, et al. MDR1 siRNA loaded hyaluronic acid-based CD44 targeted nanoparticle systems circumvent paclitaxel resistance in ovarian cancer. Sci Rep. 2015; 5:8509. [PubMed: 25687880]
20. Srinivasarao M, Galliford CV, Low PS. Principles in the design of ligand-targeted cancer therapeutics and imaging agents. Nat Rev Drug Discov. 2015; 14:1–17. DOI: 10.1038/nrd4519 [PubMed: 25503331]
21. Iyer AK, Su Y, Feng J, Lan X, Zhu X, Liu Y, Gao D, Seo Y, VanBrocklin HF, Broaddus VC, et al. The effect of internalizing human single chain antibody fragment on liposome targeting to epithelioid and sarcomatoid mesothelioma. Biomaterials. 2011; 32:2605–2613. [PubMed: 21255833]
22. Ganesh S, Iyer AK, Morrissey DV, Amiji MM. Hyaluronic acid based self-assembling nanosystems for CD44 target mediated siRNA delivery to solid tumors. Biomaterials. 2013; 34:3489–3502. DOI: 10.1016/j.biomaterials.2013.01.077 [PubMed: 23410679]
23. Boon RA, Iekushi K, Lechner S, Seeger T, Fischer A, Heydt S, Kaluza D, Tréguer K, Carmona G, Bonauer A, et al. MicroRNA-34a regulates cardiac ageing and function. Nature. 2013; 495:107–110. [PubMed: 23426265]
24. Amiji, MM., Iyer, AK. Multifunctional self-assembling polymeric nanosystems. US Pat No. 9,173,840. Nov 3. 2015 (n.d)
25. Parker N, Turk MJ, Westrick E, Lewis JD, Low PS, Leamon CP. Folate receptor expression in carcinomas and normal tissues determined by a quantitative radioligand binding assay. Anal Biochem. 2005; 338:284–93. DOI: 10.1016/j.ab.2004.12.026 [PubMed: 15745749]
26. Zwicke GL, Mansoori GA, Jeffery CJ. Utilizing the folate receptor for active targeting of cancer nanotherapeutics. Nano Rev. 2012; 3doi: 10.3402/nano.v3i0.18496
27. Padhye S, Banerjee S, Chavan D, Pandye S, Swamy KV, Ali S, Li J, Dou QP, Sarkar FH. Fluorocurcumins as cyclooxygenase-2 inhibitor: Molecular docking, pharmacokinetics and tissue distribution in mice. Pharm Res. 2009; 26:2438–2445. DOI: 10.1007/s11095-009-9955-6 [PubMed: 19714451]
28. Padhye S, Yang H, Jamadar A, Cui QC, Chavan D, Dominiak K, McKinney J, Banerjee S, Dou QP, Sarkar FH. New difluoro knoevenagel condensates of curcumin, their schiff bases and copper complexes as proteasome inhibitors and apoptosis inducers in cancer cells. Pharm Res. 2009; 26:1874–1880. DOI: 10.1007/s11095-009-9900-8 [PubMed: 19421843]

29. García-Díaz M, Nonell S, Villanueva Á, Stockert JC, Cañete M, Casadó A, Mora M, Sagristá ML. Do folate-receptor targeted liposomal photosensitizers enhance photodynamic therapy selectivity? Biochim Biophys Acta - Biomembr. 2011; 1808:1063–1071. DOI: 10.1016/j.bbamem.2010.12.014
30. Leamon CP, Low PS. Membrane folate-binding proteins are responsible for folate-protein conjugate endocytosis into cultured cells. Biochem J. 1993; 291(Pt 3):855–60. http://www.pubmedcentral.nih.gov/articlerender.fcgi?artid=1132447&tool=pmcentrez&rendertype=abstract. [PubMed: 8387781]
31. Mornet E, Carmoy N, Lainé C, Lemiègre L, Le Gall T, Laurent I, Marianowski R, Férec C, Lehn P, Benvegnu T, Montier T. Folate-equipped nanolipoplexes mediated efficient gene transfer into human epithelial cells. Int J Mol Sci. 2013; 14:1477–501. DOI: 10.3390/ijms14011477 [PubMed: 23344053]
32. Campbell IG, Jones TA, Foulkes WD, Trowsdale J. Folate-binding Protein Is a Marker for Ovarian Cancer Folate-binding Protein Is a Marker for Ovarian Cancer, (. 1991:5329–5338.
33. Phan QT, Le MH, Le TTH, Tran THH, Xuan PN, Ha PT. Characteristics and cytotoxicity of folate-modified curcumin-loaded PLA-PEG micellar nano systems with various PLA:PEG ratios. Int J Pharm. 2016; 507:32–40. DOI: 10.1016/j.ijpharm.2016.05.003 [PubMed: 27150945]
34. Zhao Y, Liu S, Li Y, Jiang W, Chang Y, Pan S, Fang X, Wang YA, Wang J. Synthesis and grafting of folate-PEG-PAMAM conjugates onto quantum dots for selective targeting of folate-receptor-positive tumor cells. J Colloid Interface Sci. 2010; 350:44–50. DOI: 10.1016/j.jcis.2010.05.035 [PubMed: 20624622]
35. Weber CJ, M??ller S, Safley SA, Gordon KB, Amancha P, Villinger F, Camp VM, Lipowska M, Sharma J, Müller C, Schibli R, Low PS, Leamon CP, Halkar RK. Expression of functional folate receptors by human parathyroid cells. Surg (United States). 2013; 154:1385–1393. DOI: 10.1016/j.surg.2013.06.045
36. Wang Y, Wang Y, Xiang J, Yao K. Target-specific cellular uptake of taxol-loaded heparin-PEG-folate nanoparticles. Biomacromolecules. 2010; 11:3531–3538. DOI: 10.1021/bm101013s [PubMed: 21086982]
37. Iyer AK, Greish K, Fang J, Murakami R, Maeda H. High-loading nanosized micelles of copoly(styrene-maleic acid)-zinc protoporphyrin for targeted delivery of a potent heme oxygenase inhibitor. Biomaterials. 2007; 28:1871–81. DOI: 10.1016/j.biomaterials.2006.11.051 [PubMed: 17208294]
38. Roy S, Yu Y, Padhye SB, Sarkar FH, Majumdar APN. Difluorinated-Curcumin (CDF) Restores PTEN Expression in Colon Cancer Cells by Down-Regulating miR-21. PLoS One. 2013; 8:5–10. DOI: 10.1371/journal.pone.0068543
39. Dandawate PR, Vyas A, Ahmad A, Banerjee S, Deshpande J, Swamy KV, Jamadar A, Dumhe-Klaire AC, Padhye S, Sarkar FH. Inclusion Complex of Novel Curcumin Analogue CDF and β-Cyclodextrin (1:2) and Its Enhanced In Vivo Anticancer Activity Against Pancreatic Cancer. Pharm Res. 2012; 29:1775–1786. DOI: 10.1007/s11095-012-0700-1 [PubMed: 22322899]
40. Anand P, Sundaram C, Jhurani S, Kunnumakkara AB, Aggarwal BB. Curcumin and cancer: an "old-age" disease with an "age-old" solution. Cancer Lett. 2008; 267:133–64. DOI: 10.1016/j.canlet.2008.03.025 [PubMed: 18462866]
41. Juliano RL, Stamp D. The effect of particle size and charge on the clearance rates of liposomes and liposome encapsulated drugs. Biochem Biophys Res Commun. 1975; 63:651–8. [PubMed: 1131256]
42. Fröhlich E. The role of surface charge in cellular uptake and cytotoxicity of medical nanoparticles. Int J Nanomedicine. 2012; 7:5577–5591. DOI: 10.2147/IJN.S36111 [PubMed: 23144561]
43. Wang L, Lu N, Zhao L, Qi C, Zhang W, Dong J, Hou X. Characterization of stress degradation products of curcumin and its two derivatives by UPLC–DAD–MS/MS. Arab J Chem. 2016
44. Luong D, Sau S, Kesharwani P, Iyer AK. Polyvalent Folate-Dendrimer-Coated Iron Oxide Theranostic Nanoparticles for Simultaneous Magnetic Resonance Imaging and Precise Cancer Cell Targeting. Biomacromolecules. 2017; 18:1197–1209. DOI: 10.1021/acs.biomac.6b01885 [PubMed: 28245646]

45. Alsaab H, Alzhrani RM, Kesharwani P, Sau S, Boddu SHS, Iyer AK. Folate Decorated Nanomicelles Loaded with a Potent Curcumin Analogue for Targeting Retinoblastoma. Pharmaceutics. 2017; 9:15.
46. Gawde KA, Kesharwani P, Sau S, Sarkar FH, Padhye S, Kashaw SK, Iyer AK. Synthesis and characterization of folate decorated albumin bio-conjugate nanoparticles loaded with a synthetic curcumin difluorinated analogue. J Colloid Interface Sci. 2017; 496:290–299. [PubMed: 28236692]
47. Xu S, Olenyuk BZ, Okamoto CT, Hamm-Alvarez SF. Targeting receptor-mediated endocytotic pathways with nanoparticles: rationale and advances. Adv Drug Deliv Rev. 2013; 65:121–138. [PubMed: 23026636]
48. Kelemen LE. The role of folate receptor $α$ in cancer development, progression and treatment: cause, consequence or innocent bystander? Int J Cancer. 2006; 119:243–250. [PubMed: 16453285]
49. Li L, Braiteh FS, Kurzrock R. Liposome-encapsulated curcumin: In vitro and in vivo effects on proliferation, apoptosis, signaling, and angiogenesis. Cancer. 2005; 104:1322–1331. DOI: 10.1002/cncr.21300 [PubMed: 16092118]
50. Bao B, Ali S, Kong D, Sarkar SH, Wang Z, Banerjee S, Aboukameel A, Padhye S, Philip PA, Sarkar FH. Anti-tumor activity of a novel compound-CDF is mediated by regulating miR-21, miR-200, and pten in pancreatic cancer. PLoS One. 2011; 6:1–12. DOI: 10.1371/journal.pone.0017850
51. Bao B, Ali S, Banerjee S, Wang Z, Logna F, Azmi AS, Kong D, Ahmad A, Li Y, Padhye S, Sarkar FH. Curcumin analogue CDF inhibits pancreatic tumor growth by switching on suppressor microRNAs and attenuating EZH2 expression. Cancer Res. 2012; 72:335–345. DOI: 10.1158/0008-5472.CAN-11-2182 [PubMed: 22108826]
52. Nagata Y, Lan KH, Zhou X, Tan M, Esteva FJ, Sahin AA, Klos KS, Li P, Monia BP, Nguyen NT, Hortobagyi GN, Hung MC, Yu D. PTEN activation contributes to tumor inhibition by trastuzumab, and loss of PTEN predicts trastuzumab resistance in patients. Cancer Cell. 2004; 6:117–127. DOI: 10.1016/j.ccr.2004.06.022 [PubMed: 15324695]
53. Ruutu M, Peitsaro P, Johansson B, Syrjänen S. Transcriptional profiling of a human papillomavirus 33-positive squamous epithelial cell line which acquired a selective growth advantage after viral integration. Int J Cancer. 2002; 100:318–326. DOI: 10.1002/ijc.10455 [PubMed: 12115547]
54. Baeuerle PA, Baltimore D. Nf-κB: Ten years after. Cell. 1996; 87:13–20. DOI: 10.1016/S0092-8674(00)81318-5 [PubMed: 8858144]
55. Fontaine V, van der Meijden E, de Graaf J, ter Schegget J, Struyk L. A functional NF-κB binding site in the human papillomavirus type 16 long control region. Virology. 2000; 272:40–49. DOI: 10.1006/viro.2000.0363 [PubMed: 10873747]
56. Spitkovsky D, Hehner SP, Hofmann TG, Moller A, Schmitz ML. The human papillomavirus oncoprotein E7 attenuates NF-kappa B activation by targeting the Ikappa B kinase complex. J Biol Chem. 2002; 277:25576–25582. DOI: 10.1074/jbc.M201884200 [PubMed: 11986318]
57. Patel D, Huang SM, Baglia LA, McCance DJ, Nees M, Geoghegan JM, Hyman T, Frank S, Miller L, Woodworth CD. The E6 protein of human papillomavirus type 16 binds to and inhibits co-activation by CBP and p300. EMBO J. 1999; 18:5061–5072. DOI: 10.1093/emboj/18.18.5061 [PubMed: 10487758]
58. Nees M, Geoghegan JM, Hyman T, Frank S, Miller L, Woodworth CD. Papillomavirus type 16 oncogenes downregulate expression of interferon-responsive genes and upregulate proliferation-associated and NF-kappaB-responsive genes in cervical keratinocytes. J Virol. 2001; 75:4283–4296. DOI: 10.1128/JVI.75.9.4283-4296.2001 [PubMed: 11287578]

Research highlights

- Folic acid (FA) is a well-established biomarker for folate overexpressing cancers.
- A new FA linked block-copolymer with styrene malic acid (FA-SMA) is reported.
- FA-SMA forms nanomicelles with a potent difluorinated curucumin analog (CDF).
- FA-SMA-CDF shows promising potential on cervical and ovarian cancers

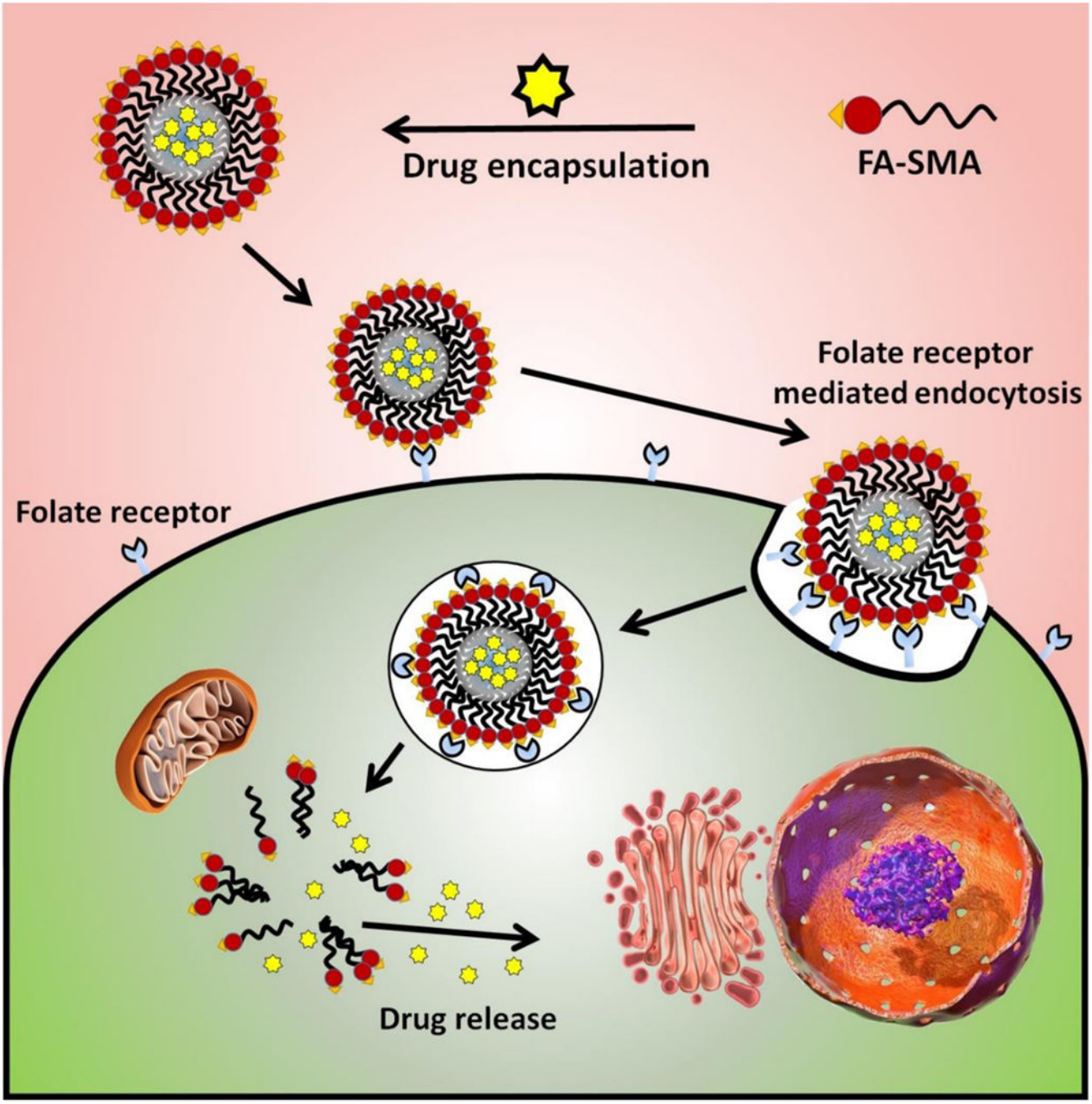

Figure 1.

The pictorial representation of accumulation of targeted nanomicelles (FA-SMA-CDF) at the tumor site by folate receptor-mediated endocytosis due to the specific binding of FA to folate receptors overexpressed on cancer cells is shown.

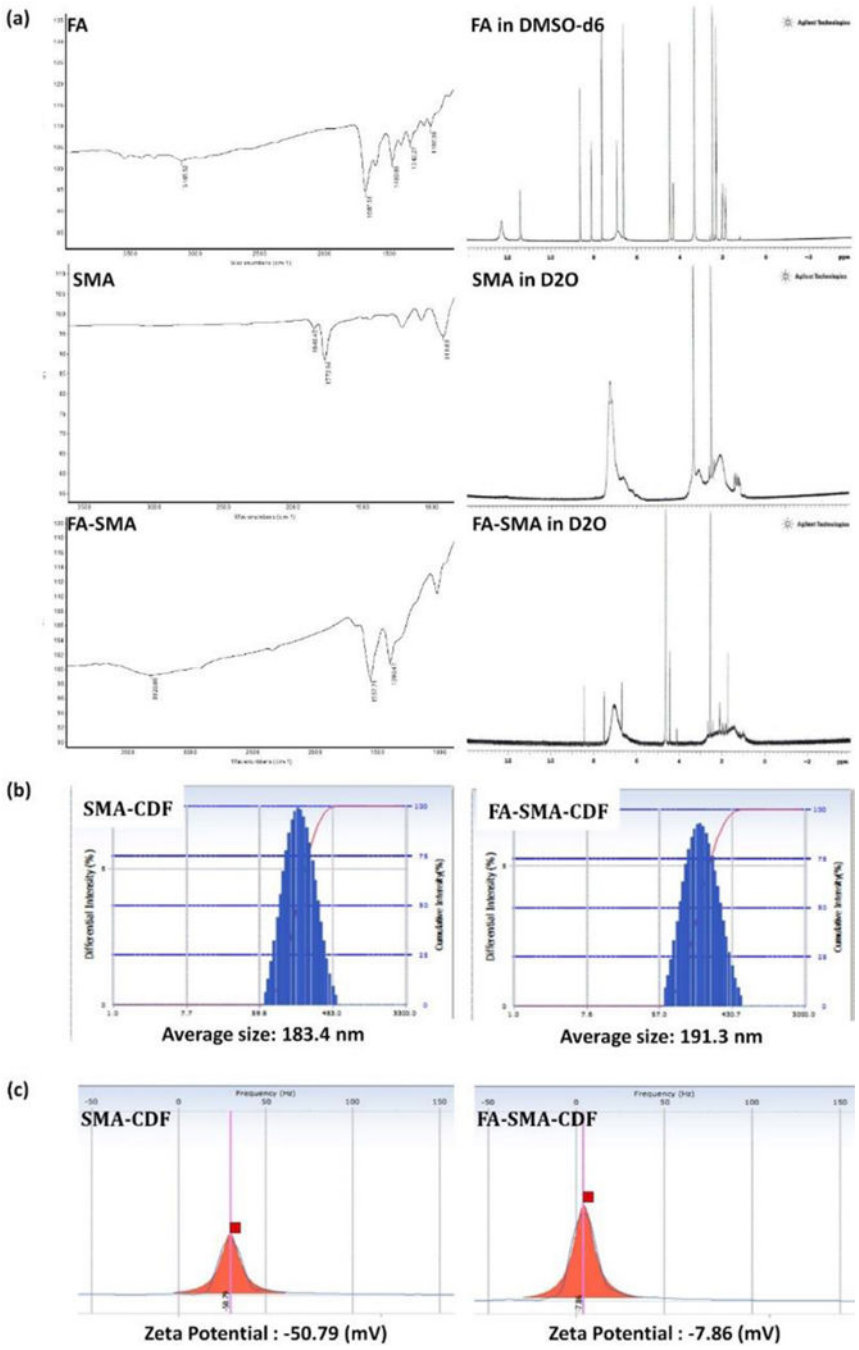

Figure 2.

(a) FTIR (left) and ^{1}H NMR (right) characterization of FA, SMA, and FA-SMA conjugate; (b) Particle size and (c) Zeta potential characterization of SMA-CDF and FA-SMA-CDF using Dynamic light scattering (DLS) technique.

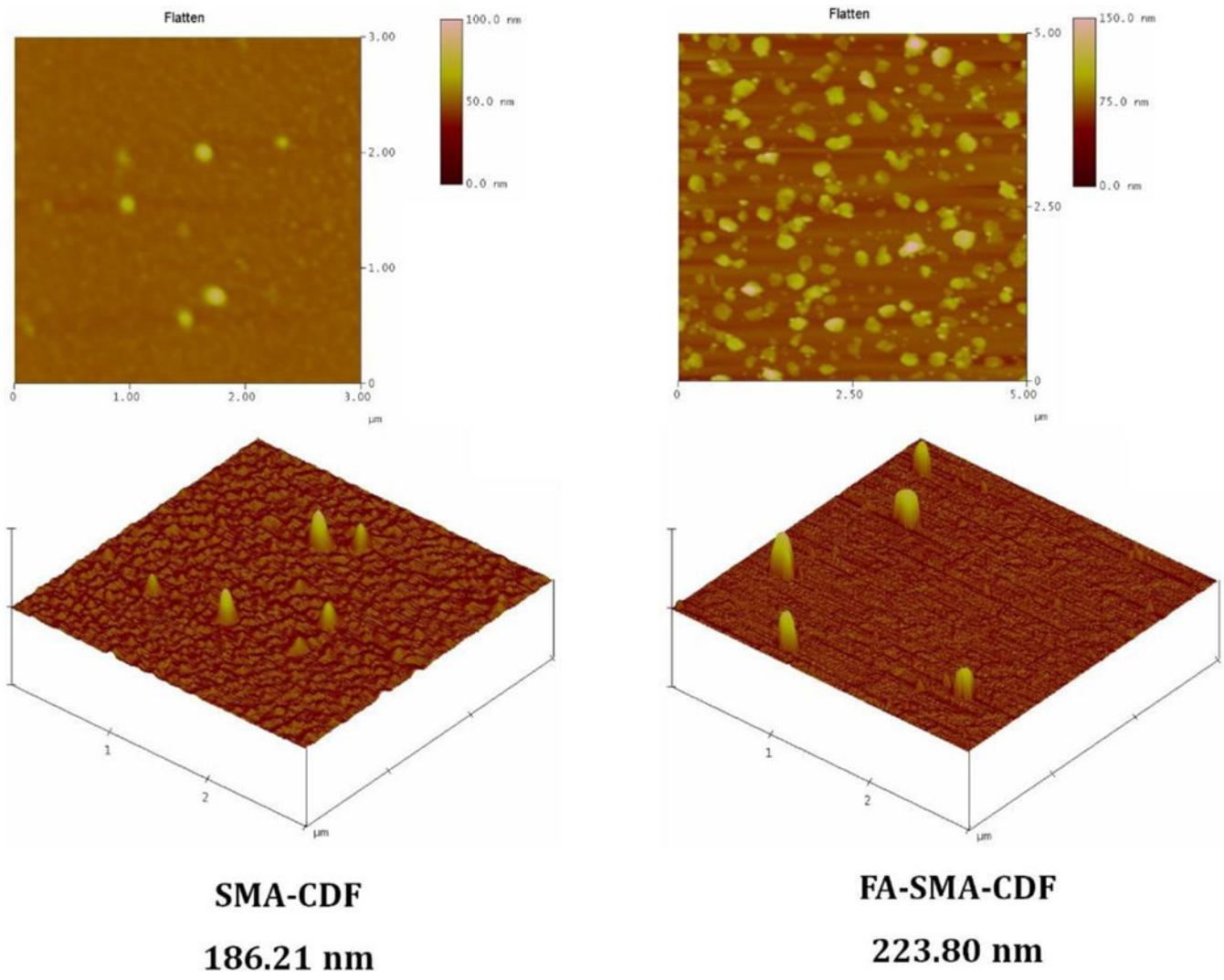

Figure 3.
Surface morphology of SMA-CDF and FA-SMA-CDF by Atomic force microscopy (AFM).

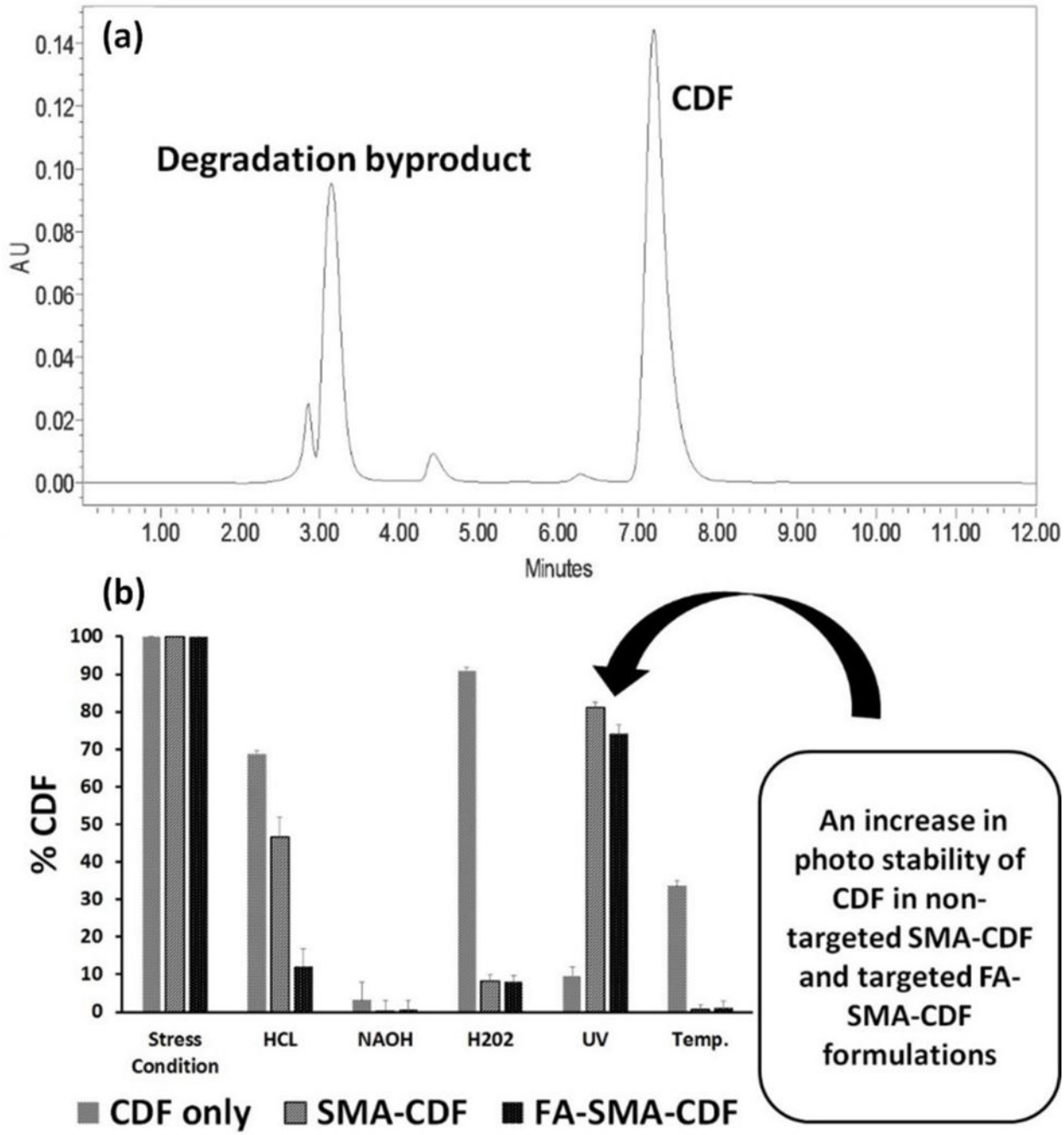

Figure 4.

(a) HPLC analysis. There is no interference in HPLC between drug peak and the degradation peaks; (b) Stability of nanomicelles under varying conditions are shown. It can be seen that the nano micellar formulation of CDF increased the drug photolytic stability significantly (n=3).

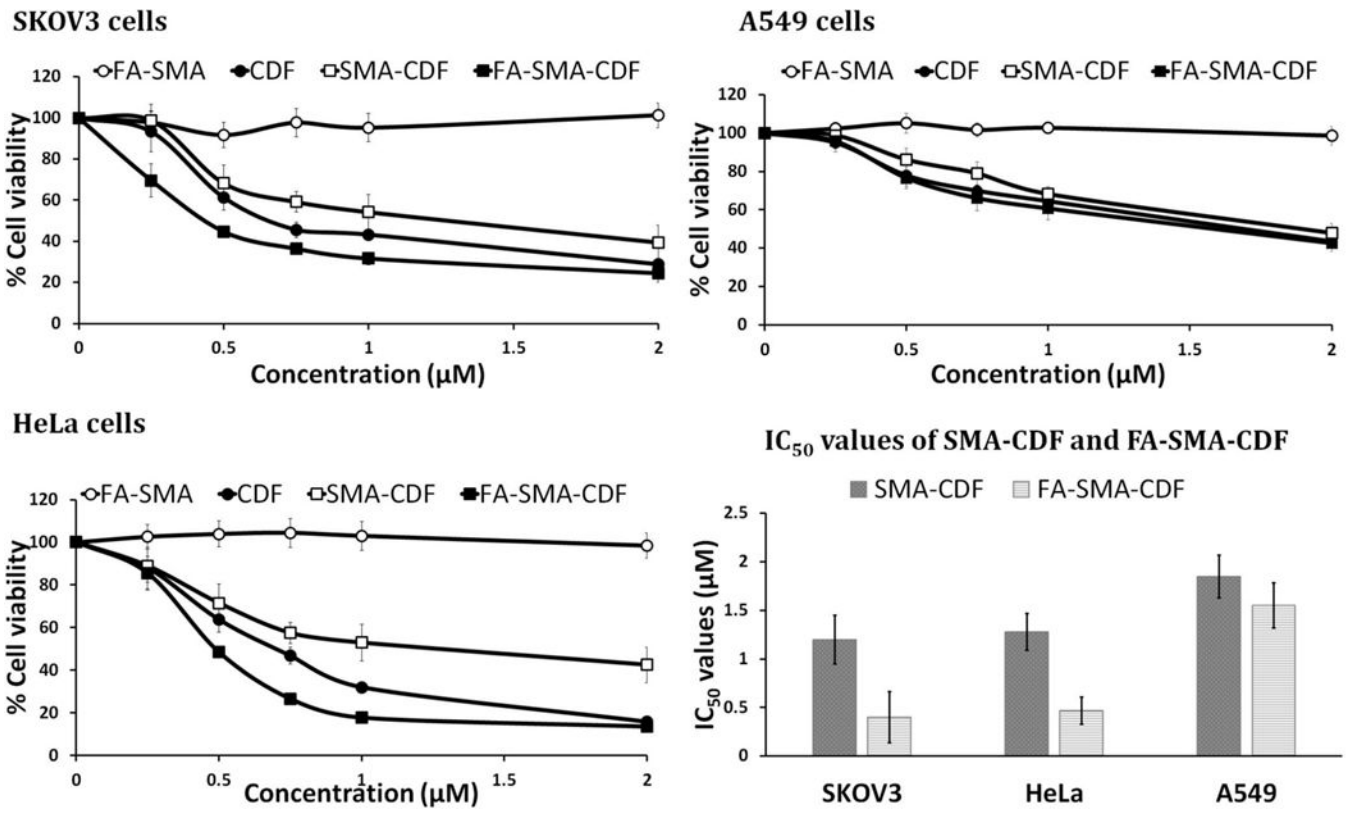

Figure 5.

In vitro cell viability assay showing the percentage of cell viability and the IC_{50} values observed at 72 h after treating SKOV3, HeLa and A549 cells with various formulations are shown (n=8).

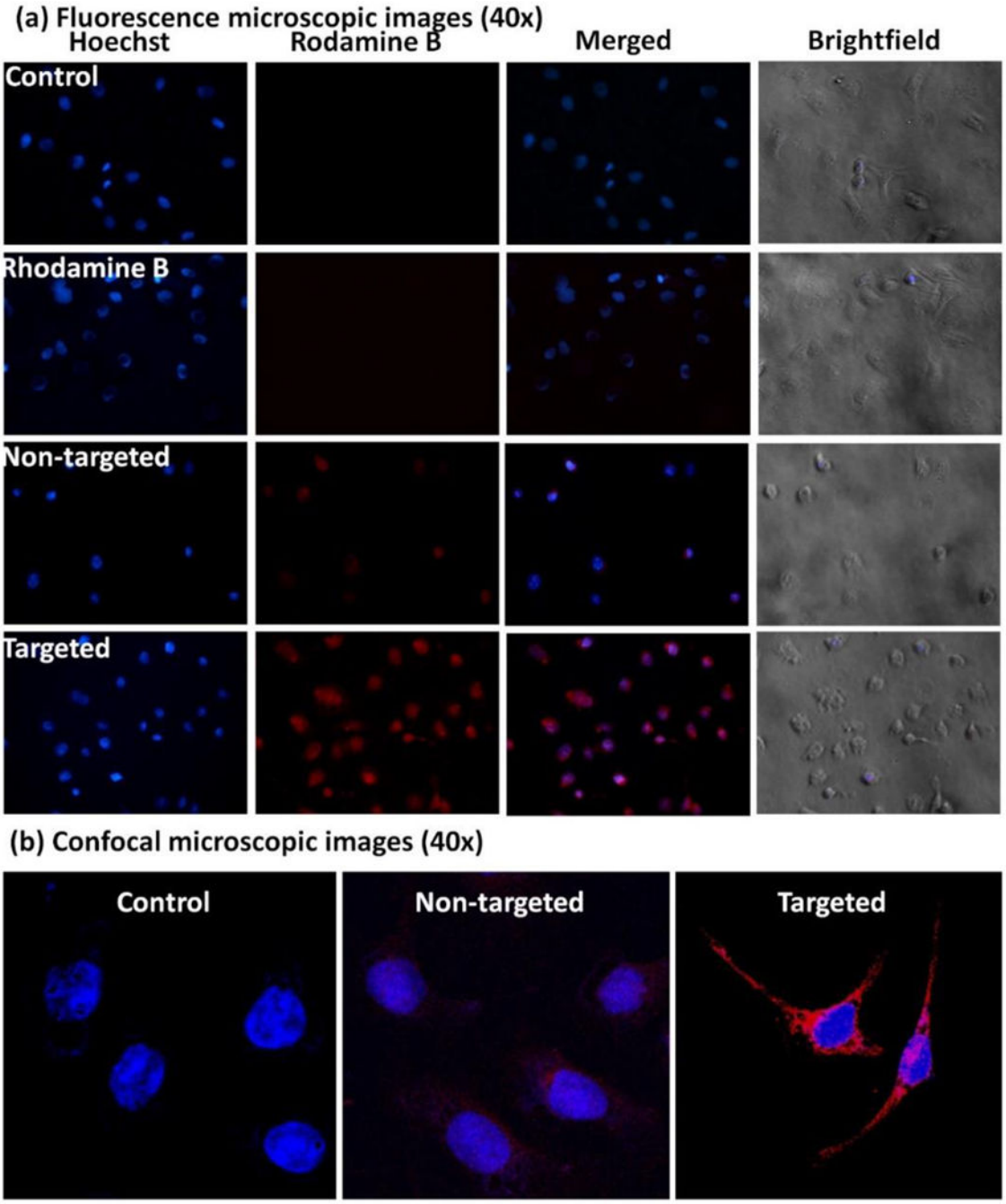

Figure 6.

(a) Fluorescence microscopic images (40×) of SKOV3 cells incubated with nuclear stain Hoechst (blue fluorescence) and Rhodamine B (red fluorescence) labeled non-targeted and targeted formulations at 6 h are shown; (b) Confocal images of SKOV3 cells treated with DRAQ5® stain alone (control, blue fluorescence) or DRAQ5 and Rhodamine B (red fluorescence) labeled non-targeted formulation, and targeted formulation respectively are shown. Higher cellular uptake of the targeted formulation is suggested by the higher red fluorescent signal of Rhodamine B.

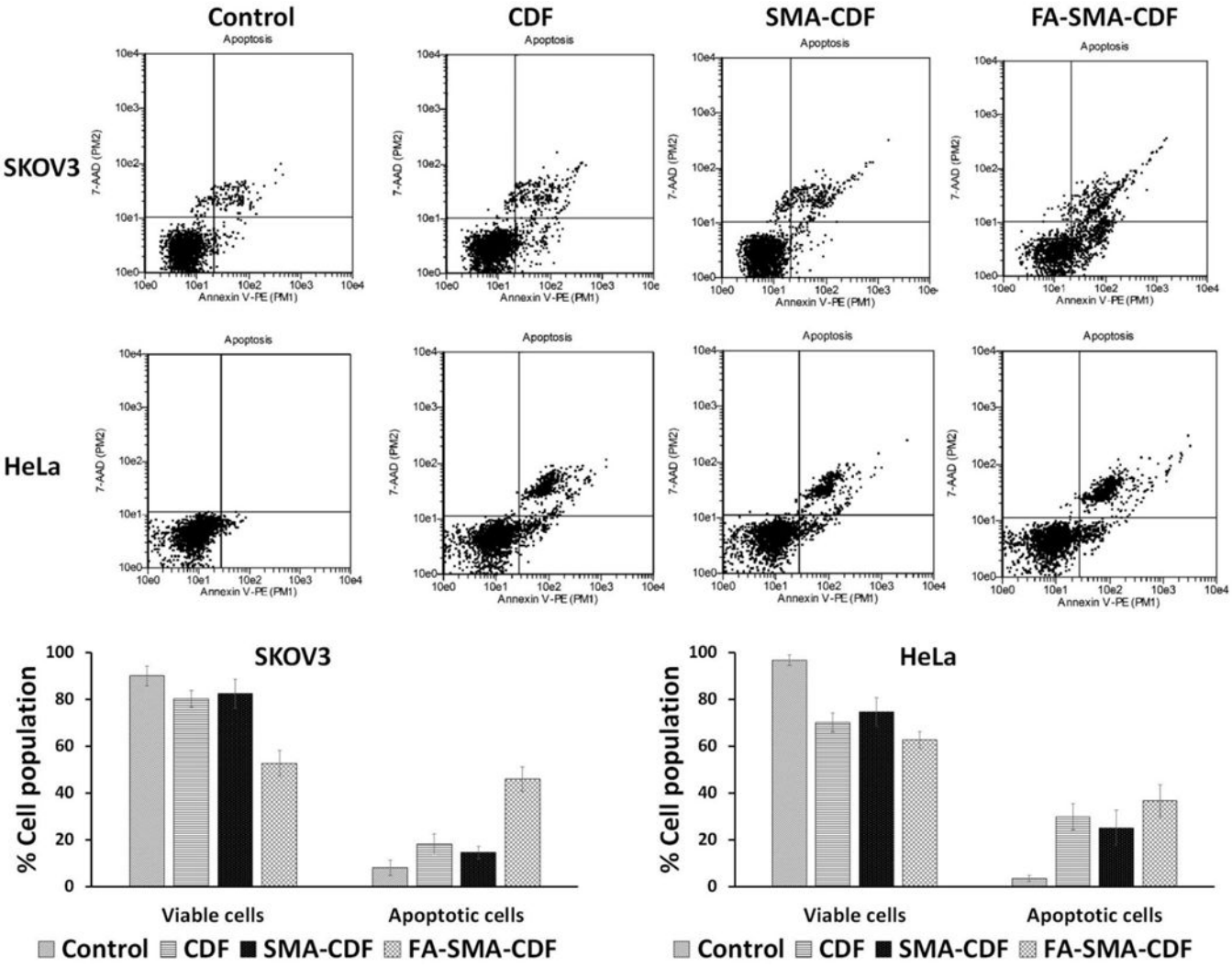

Figure 7.

Induction of apoptosis in SKOV3 and HeLa cells when treated with CDF, SMA-CDF, and FA-SMA-CDF as evaluated by Annexin V/7-AAD dual staining. An increased percentage of the apoptotic cell population was noted when cells were treated with targeted formulation (FA-SMA-CDF) as compared to both plain CDF and non-targeted SMA-CDF, suggesting the better killing activity of the targeted formulation FA-SMA-CDF (n=3).

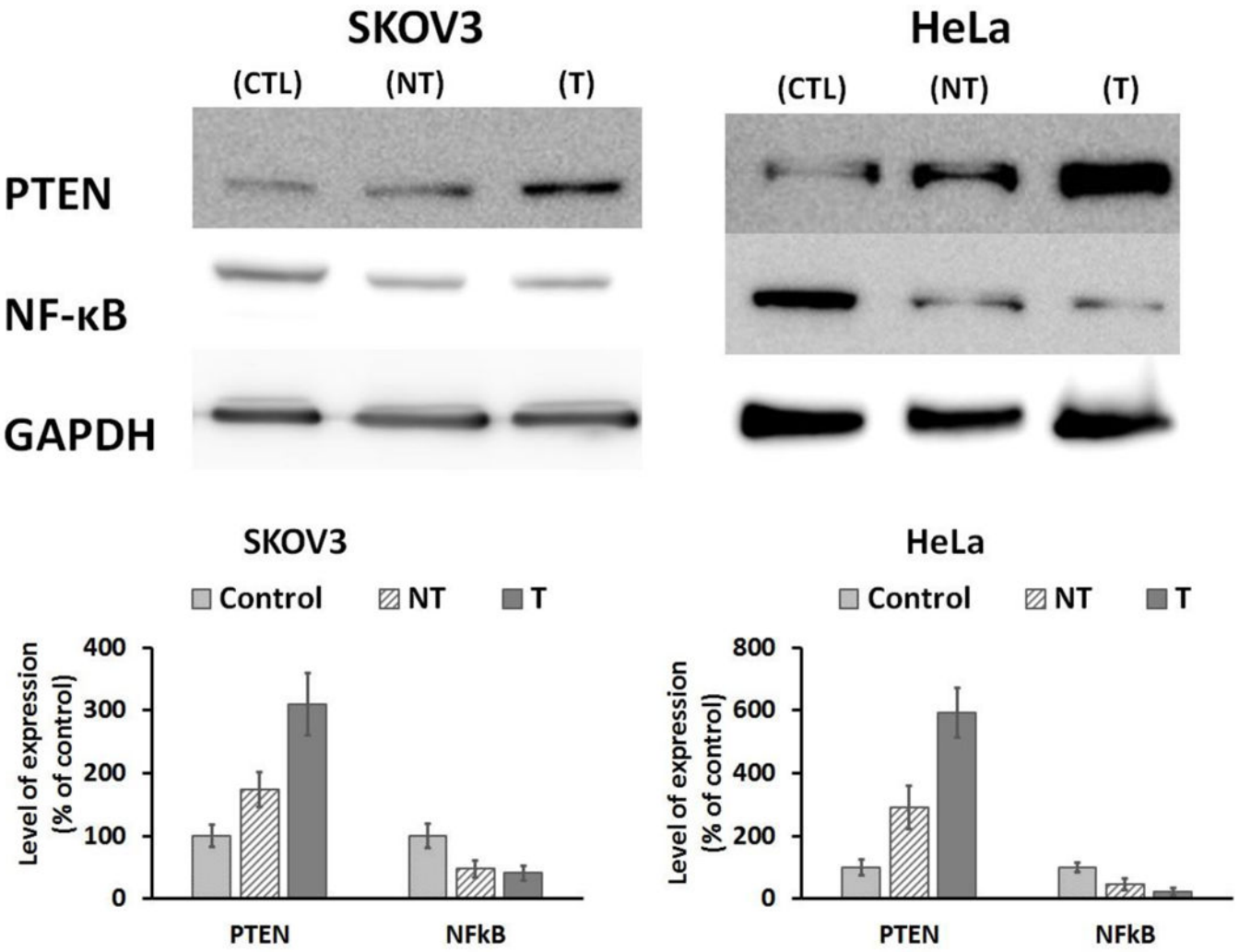

Figure 8.

Western blot analysis showing PTEN and NF-κB expression in SKOV3 and HeLa cells without treatment as controls (CTL), and in SKOV3 and HeLa cells after treatment with SMA-CDF (NT) and FA-SMA-CDF (T) (GAPDH expression was used as the protein loading control, n =3).